



Synthesis, characterisation and biological activity of Co(III) complex with the condensation product of 2-(diphenylphosphino)benzaldehyde and ethyl carbazate

Milica Milenković^a, Alessia Bacchi^b, Giulia Cantoni^b, Siniša Radulović^c, Nevenka Gligorijević^c, Sandra Arandelović^c, Dušan Sladić^a, Miroslava Vujčić^d, Dragana Mitić^a, Katarina Anđelković^{a,*}

^a Faculty of Chemistry, University of Belgrade, Studentski trg 12-16, 11000 Belgrade, Serbia

^b Dipartimento di Chimica Generale ed Inorganica, Chimica Analitica, Chimica Fisica, University of Parma, Parco Area delle Scienze 17 A, I 43100 Parma, Italy

^c Institute for Oncology and Radiology of Serbia, Department of Experimental Oncology, Laboratory for Experimental Pharmacology, Pasterova 14, Belgrade, Serbia

^d Institute of Chemistry, Technology and Metallurgy, University of Belgrade, Njegoševa 12, P.O. Box 815, 11000 Belgrade, Serbia

ARTICLE INFO

Article history:

Received 15 June 2012

Received in revised form 27 September 2012

Accepted 29 September 2012

Available online 2 November 2012

Keywords:

Cobalt(III) complex

X-ray

Antitumor activity

Antimicrobial activity

DNA binding

ABSTRACT

A cobalt(III) complex with the condensation derivative of 2-(diphenylphosphino)benzaldehyde and ethyl carbazate was synthesized. X-ray crystal structure was determined for both the ligand and the complex. In the cobalt(III) complex two deprotonated ligand molecules coordinate the metal atom in a distorted octahedral geometry by chelation through the PNO donor system formed by the phosphorus, the imine nitrogen and the carbonyl oxygen. The complex showed a moderate antibacterial activity and a strong cytotoxic activity, stronger than cisplatin. Based on cell cycle progression, apoptotic assays, spectroscopic and electrophoretic studies, it was shown that high cytotoxicity and moderate potential of induction of apoptosis are not consequence of interactions with DNA.

© 2012 Elsevier B.V. All rights reserved.

1. Introduction

The design and synthesis of multidentate ligands which are derivatives of 2-(diphenylphosphino)benzaldehyde continue to be an important research area in coordination chemistry. Derivatives with 'soft' phosphorus and 'hard' nitrogen donor atoms are of particular interest in catalytic processes [1–3]. The incorporation of a chiral centre into complexes of these ligands allows enantioselectivity in catalytic transformations mediated by these compounds [4–10]. Complexes of nickel(II) and copper(I) with condensation derivatives of 2-(diphenylphosphino)benzaldehyde and semicarbazide, thiosemicarbazide or selenosemicarbazide were synthesized. These ligands are coordinated as tridentates via PNO, PNS or PNSe donor atom sets [11–14]. Square-planar Pd(II) and Ni(II) complexes with condensation derivatives of 2-(diphenylphosphino)benzaldehyde and different hydrazides coordinated as tridentates via PNO donor atom sets show a significant catalytic activity [15–17]. The catalytic properties of nickel(II) acetato complex of 2-(diphenylphosphino)benzaldehyde 2-pyridylhydrazone with PNN set of donor atoms were also studied

[17]. The number of papers dealing with biological activity of derivatives of 2-(diphenylphosphino)benzaldehyde and their metal complexes is much smaller.

Complexes of Pt(II), Pd(II), and Ni(II) with the condensation derivative of 2-(diphenylphosphino)benzaldehyde and semioxamazide were synthesized with the aim to obtain biologically active compounds. The ligand showed antibacterial and antifungal activity, which was enhanced upon complexation [18].

Palladium(II) complex with the condensation product of 2-(diphenylphosphino)benzaldehyde and ethyl hydrazinoacetate exhibits a similar effect to cisplatin on HeLa cells, inducing apoptosis followed by arrest of cells in S phase of cell cycle, while complexes of platinum(II) and palladium(II) with the condensation product of 2-(diphenylphosphino)benzaldehyde and semioxamazide induce apoptosis in HeLa cells without significant perturbations of cell cycle distribution. Complexes of platinum(II) and palladium(II) with the condensation product of 2-(diphenylphosphino)benzaldehyde and semioxamazide showed a strong cytotoxicity to CDDP-resistant U2-OS/Pt cells [19].

The subject of this work was the synthesis, characterization and preliminary evaluation of the biological activity of Co(III) complex with a ligand which is the condensation derivative of 2-(diphenylphosphino)benzaldehyde and ethyl carbazate.

* Corresponding author.

E-mail address: kka@chem.bg.ac.rs (K. Anđelković).

This is a continuation of the study of complexes with this type of ligands, in which our attention was shifted to complexes with potential octahedral geometry, with the aim to get information on influence of structure on activity. Ethyl carbazate was selected as the hydrazine part of the ligand instead of ethyl hydrazinoacetate, since the latter would not be able to form a five-membered ring suitable for coordination of the ligand as a tridentate.

2. Experimental

2.1. Material and methods

2-(Diphenylphosphino)benzaldehyde (97%) and ethyl carbazate (97%) were obtained from Aldrich. IR spectra were recorded on a Perkin-Elmer FT-IR 1725X spectrometer using the ATR technique in the region 4000–400 cm^{-1} . ^1H NMR (500 MHz), ^{13}C NMR (125 MHz) and 2D NMR spectra were recorded on a Bruker Avance 500 spectrometer in $\text{DMSO}-d_6$ using TMS as internal standard for ^1H and ^{13}C . All spectra were measured at 25 °C. **1** and **2** were characterized on the basis of NMR spectroscopy results: 1D (^1H , ^{13}C , DEPT), 2D (COSY, NOESY) as well as 2D ^1H – ^{13}C heteronuclear correlation spectra (HSQC). Mass spectrum for **1** was taken on a 6210 TOF LC/MS coupled with an Agilent Technologies 1200 Series HPLC system. Elemental analyses (C, H, and N) were performed by standard micro-methods using the ELEMENTARVario ELIII C.H.N.S.O analyzer.

2.1.1. Synthesis of ethyl (2E)-2-[2-(diphenylphosphino)benzylidene]hydrazinecarboxylate (**1**)

A mixture of 0.14 g (0.48 mmol) 2-(diphenylphosphino)benzaldehyde and 0.05 g (0.48 mmol) ethyl carbazate was dissolved, by heating, in 25 mL ethanol. pH of the mixture was adjusted to ~4 with a hydrochloric acid. The mixture was heated at 56 °C for 60 min. The reaction solution was left to stand at room temperature while the colourless crystals separated from the solution. Yield 0.15 g (83%). Mp 164–166 °C. IR (vs-very strong, s-strong, m-medium, w-weak): 3253 (w), 3189 (w), 3049 (m), 2974 (w), 1729 (m), 1707 (s), 1550 (s), 1458 (w), 1435 (w), 1385 (w), 1247 (vs), 1178 (w), 1092 (w), 1055 (m), 763 (w), 744 (w), 696 (m), 657 (w), 499 (w). HRMS (ESI) of $\text{C}_{22}\text{H}_{21}\text{N}_2\text{O}_2\text{P}$ found for $(\text{M}+\text{H}^+)$ 377.1384, calcd (m/z) for $(\text{M}+\text{H}^+)$ 377.1414.

2.1.2. Synthesis of Co(III) complex (**2**)

A mixture of 0.24 g (0.64 mmol) of the ligand and 0.13 g (0.38 mmol) $\text{Co}(\text{BF}_4)_2 \cdot 6\text{H}_2\text{O}$ was dissolved, by heating, in 25 mL ethanol. The mixture was heated at 56 °C for 6 h. The color of the solution changed to dark red. The reaction solution was left to stand at room temperature. Dark red crystals were obtained from the reaction solution. Yield 0.08 g (23.4%). IR (vs-very strong, s-strong, m-medium, w-weak): 3079 (w), 2981 (w), 1507 (vs), 1480 (vs), 1429 (vs), 1379 (m), 1337 (vs), 1060 (s), 750 (m), 701 (m), 659 (w), 611 (m). Elemental analysis for $\text{C}_{44}\text{H}_{40}\text{BCoF}_4\text{N}_4\text{O}_4\text{P}_2$. Anal. Calc. N 6.25, C 58.95, H 4.50%. Found: N 6.05, C 58.82, H 4.63%.

2.2. Crystallographic structure determination

Single crystal X-ray diffraction data were collected at $T = 293\text{ K}$ using the Mo $\text{K}\alpha$ radiation ($\lambda = 0.71073\text{ \AA}$) on a SMART APEX2 diffractometer for **2** and on a Siemens AED diffractometer equipped with scintillation detector and Cu $\text{K}\alpha$ radiation ($\lambda = 1.54178\text{ \AA}$) for **1**. Lorentz, polarization, and absorption corrections were applied [20]. Structures were solved by direct methods using SIR97 [21] and refined by full-matrix least-squares on all F^2 using SHELXL97 [22] implemented in the WinGX package [23]. Hydrogen atoms were introduced in calculated positions apart from NH hydrogens

in **1** that were found on difference maps and refined. Anisotropic displacement parameters were refined for all non-hydrogen atoms. The BF_4^- anion in **2** is disordered and has been modeled over two images with 0.7:0.3 population. Hydrogen bonds have been analyzed with SHELXL97 [22] and PARST97 [23] and extensive use was made of the Cambridge Crystallographic Data Centre packages [24] for the analysis of crystal packing. Table 1 summarizes crystal data and structure determination results.

2.3. Antimicrobial activity

The antimicrobial activity was evaluated using seven different laboratory control strains of bacteria, i.e., the Gram-positive: *Staphylococcus aureus* (ATCC 25923), *Staphylococcus epidermidis* (ATCC12228), *Kocuria rhizophila* (ATCC 9341), *Bacillus subtilis* (ATCC 6633) and the Gram-negative: *Escherichia coli* (ATCC 25922), *Klebsiella pneumoniae* (ATCC 13883), *Pseudomonas aeruginosa* (ATCC 27853), and two strains of yeast, i.e., *Candida albicans* (ATCC 10259 and ATCC 10231). All tests were performed in Müller Hinton broth for the bacterial strains and in Sabouraud dextrose broth for the yeast. Overnight broth cultures of each strain were prepared, and the final concentration in each well was adjusted to $2 \times 10^6\text{ CFU ml}^{-1}$ for the bacteria and $2 \times 10^5\text{ CFU ml}^{-1}$ for the yeast. The investigated compounds were dissolved in 1% dimethyl sulfoxide (DMSO) and then diluted to the highest concentration. Twofold serial concentrations of the compounds were prepared in a 96-well microtiter plate over the concentration range 31.25–500 $\mu\text{g ml}^{-1}$. The microbial growth was determined after 24 h incubation at 37 °C for the bacteria and after 48 h incubation at 26 °C for the fungi. The MIC is defined as the lowest concentration of the compound at which no visible growth of microorganism is observed.

2.4. The brine shrimp test

A teaspoon of lyophilized eggs of the brine shrimp *Artemia salina* was added to 0.5 L of the artificial sea water containing several drops of yeast suspension (3 mg of dry yeast in 5 mL distilled water), and air was passed through the suspension thermostated at 18–20 °C, under illumination for 48 h. Hatched nauplii were used in further experiments.

In a glass vial, into 1 mL of artificial sea water 1–2 drops of yeast extract solution (3 mg in 5 mL of distilled water) and 10–20 hatched nauplii were added, and finally water solution of $\text{Co}(\text{BF}_4)_2 \cdot 6\text{H}_2\text{O}$ to the appropriate concentrations. The substances **1** and **2** were dissolved in DMSO and then in various amounts applied to paper discs 2 cm in diameter. Paper discs were placed on the bottom of the glass vial into which was added 5 mL of artificial sea water, 1–2 drops of yeast suspension, and about 15–20 hatched nauplii.

The vials were left at room temperature under illumination for 24 h, and afterwards live and dead nauplii were counted. LC_{50} was defined as the concentration of substances that causes death of 50% nauplii.

2.5. Cytotoxic activity

2.5.1. Cell culture

Human cervix carcinoma cells (HeLa), human melanoma cells (FemX), human colon cancer cells (LS-174) and human fetal lung fibroblast cells (MRC-5) were maintained as monolayer culture in nutrient medium (the RPMI 1640 medium). Powdered RPMI 1640 medium, was purchased from Sigma Aldrich Co. Nutrient medium RPMI 1640 was prepared in sterile ionized water, supplemented with penicillin (192 IU/mL), streptomycin (200 $\mu\text{g/mL}$), 4-(2-hydroxyethyl)piperazine-1-ethanesulfonic acid (HEPES) (25 mM), L-glutamine (3 mM) and 10% of heat-inactivated fetal calf serum

Table 1
Crystal data and structure refinement for **1** and **2**.

	1	2
Empirical formula	C ₄₄ H ₄₂ N ₄ O ₄ P ₂	C ₄₄ H ₄₀ N ₄ O ₄ P ₂ CoBF ₄
Formula weight	752.76	896.48
Temperature (K)	293(2)	293(2)
Crystal system	monoclinic	monoclinic
Space group	<i>I</i> 2/a	<i>P</i> 2 ₁ /n
<i>a</i> (Å)	24.584(3)	15.677(1)
<i>b</i> (Å)	9.2487(4)	13.403(1)
<i>c</i> (Å)	36.028(2)	19.949(2)
β (°)	98.297(6)	93.012(1)
Volume (Å ³)	8106(1)	4185.9(6)
<i>Z</i>	8	4
ρ_{calc} (mg/mm ³)	1.234	1.423
μ (mm ⁻¹)	1.347	0.553
<i>F</i> (000)	3168.0	1848.0
2 θ range for data collection	7.26–139.84°	3.22–63.98°
Reflections collected	14815	68322
Independent reflections	7669	13805
	[<i>R</i> _{int} = 0.0297]	[<i>R</i> _{int} = 0.0284]
Data/restraints/parameters	7669/0/498	13805/0/569
Goodness-of-fit (GOF) on <i>F</i> ²	1.035	1.029
Final <i>R</i> ₁ , <i>wR</i> ₂ [<i>I</i> > 2 σ (<i>I</i>)]	0.0425, 0.1219	0.0386, 0.1053
Final <i>R</i> ₁ , <i>wR</i> ₂ [all data]	0.0452, 0.1247	0.0535, 0.1150
Largest ΔF maximum/minimum (e Å ⁻³)	0.51/–0.28	0.57/–0.45

Table 2
Results of MTT assay after 48 h agent action.

	IC ₅₀ (μM)			
	HeLa	FemX	LS-174	MRC-5
(1)	58.28 ± 0.23	>100	>100	>100
(2)	4.90 ± 0.08	6.45 ± 1.85	7.42 ± 2.45	7.42 ± 0.05
Co(BF ₄) ₂ ·6H ₂ O	72.04 ± 6.83	82.11 ± 2.95	94.29 ± 5.05	77.27 ± 1.29
CDDP	7.79 ± 2.32	10.77 ± 0.88	22.41 ± 7.18	30.26 ± 2.98

(FCS) (pH 7.2). The cells were grown at 37 °C in 5% CO₂ and humidified air atmosphere, by twice weekly subculture.

2.5.2. MTT assay

Cytotoxicity of the investigated cobalt(III) complex (**2**), the ligand (**1**) and cobalt salt in comparison to cisplatin, was determined using the 3-(4,5-dimethylthiazol-2-yl)-2,5-diphenyltetrazolium bromide (MTT, Sigma) assay [25]. Cells were seeded in 96-well cell culture plates (Linbro), HeLa (3000 c/w), FemX (5000 c/w), LS-174 (7000 c/w) and MRC-5 (5000 c/w) in culture medium and grown for 24 h. Stock solutions of investigated agents were made in DMSO at concentration of 10 mM, and afterwards diluted with nutrient medium to desired final concentrations (in range up to 100 μM). Cisplatin (CDDP) stock solution was made in 0.9% NaCl at concentration of 10 mM and afterwards diluted with nutrient medium to desired final concentrations (in range up to 100 μM). Solutions of various concentrations of the examined compounds were added to the wells, except the control wells where only nutrient medium was added. All samples were done in triplicate. Nutrient medium with corresponding agent concentrations but without target cells, was used as a blank, also in triplicate.

Cells were incubated for 48 h with the test compounds at 37 °C, with 5% CO₂ in humidified atmosphere. After incubation, 20 μL of MTT solution, 5 mg/mL in phosphate buffer solution (PBS), pH 7.2, were added to each well. Samples were incubated for 4 h at 37 °C with 5% CO₂ in humidified atmosphere. Formazan crystals were dissolved in 100 μL 10% sodium dodecyl sulfate (SDS) in 0.01 M HCl. Absorbance was recorded on the ThermoLabsystems 408 Multiskan EX 200–240 V after 24 h at a wavelength of 570 nm. Concentration IC₅₀ (μM) was defined as the concentration

of drug producing 50% inhibition of cell survival. It is determined from the cell survival diagrams.

2.5.3. Cell cycle analysis

Quantitative analysis of cell cycle phase distribution was performed by flow-cytometric analysis of the DNA content in fixed HeLa cells, after staining with propidium iodide (PI) [26].

Cells were seeded at density of 2 × 10⁵ cells/well at 6-well plate and grown in nutrition medium. After 24 h cells were continually exposed to investigated cobalt(III) complex (**2**) with concentrations that correspond to 0.5xIC₅₀ and IC₅₀ (determined for 48 h treatment Table 2). Control cells were incubated only in nutrient medium, and as reference compound cisplatin was used. After 24 and 48 h of continual treatment cells were collected by trypsinization, washed twice with ice-cold PBS, and fixed for 30 min in 70% EtOH. After fixation cells were washed again with PBS, and incubated with RNaseA (1 mg/ml) for 30 min at 37 °C. Cells were then stained with PI (at concentration of 400 μg/ml) 15 min before flow-cytometric analysis. Cell cycle phase distribution were analyzed using a fluorescence activated sorting cells (FACS) Calibur Becton Dickinson flow cytometer and Cell Quest Pro computer software.

2.5.4. Apoptotic assay

Induction of apoptosis by cobalt(III) complex (**2**) and cisplatin (CDDP) in HeLa cells was evaluated by Annexin V-FITC apoptosis detection kit (BD Biosciences Cat. No. 65874x, Pharmingen San Diego, CA, USA). Briefly, 1 × 10⁶ HeLa cells/mL were treated with 0.5 × IC₅₀ and IC₅₀ concentrations of cobalt(III) complex and CDDP (see Table 2) for 48 h. After treatment cells were washed twice with cold PBS and then resuspended in 200 μL binding buffer (10 mM HEPES/NaOH pH 7.4, 140 mM NaCl, 2.5 mM CaCl₂). 100 μL of the solution (1 × 10⁵ cells) was transferred to a 5 mL culture tube and 2.5 μL of Annexin V-FITC and 2.5 μL of PI was added. Cells were gently vortexed and incubated for 15 min at 25 °C in the dark. After that 400 μL of binding buffer was added to each tube and then analysed using a FACS Calibur Becton Dickinson flow cytometer and Cell Quest Pro computer software.

2.6. DNA binding experiments

2.6.1. Interaction of the Co(III) complex (**2**) with double stranded closed circular plasmid DNA

Plasmid pUC18 was prepared by transformation of a clone from *Escherichia coli* RR1 (pUC18, 2686 bp, purchased from Sigma-Aldrich, USA) into electrocompetent *E. coli* DH5 α strain cells according to the protocol for growing *E. coli* culture overnight in LB medium at 37 °C by electroporation with the “Gene Pulser” (Bio-Rad) [27]. The plasmid DNA from *E. coli* clones were isolated by modified method of alkali lysis [28] and purified with the “JetStar” kit (Genomed) using anion-exchange column. After final washing step with ice-cold 70% ethanol, DNA pellet was air-dried and finally resuspended in 150 μL sterile H₂O and stored at –20 °C. The concentration of plasmid DNA (213 ng/μL of pUC18) was determined by measuring the absorbance of the DNA-containing solution at 260 nm. One optical unit corresponds to 50 μg/mL of double stranded DNA.

Plasmid DNA was incubated for 4 min at 95 °C, followed by incubation at 4 °C for the next 20 min. Then 213 ng (0.13 pmol) of pUC18 in a 20 μL reaction mixtures in TS buffer (20 mM Tris 20 mM NaCl, pH 7.92), were incubated with different concentration (5 nmol, 10 nmol or 15 nmol) of the complex at 37 °C, for 1.5 h. The control sample was prepared with 3 μL of DMSO instead of complex. The reaction mixtures were vortexed from time to time. The reaction was terminated by short centrifugation at 10000 rpm and adding 7 μL of loading buffer (0.25% bromophenol blue, 0.25% xylene cyanol FF and 30% glycerol in TAE buffer, pH

8.24 (40 mM Tris–acetate, 1 mM EDTA)). The samples were subjected to electrophoresis on 1% agarose gel (Amersham Pharmacia-Biotech, Inc., USA) prepared in TAE buffer pH 8.24. The electrophoresis was performed at a constant voltage (80 V) for 1.5 h (until bromophenol blue had passed through 75% of the gel). After electrophoresis, the gel was stained for 30 min by soaking it in an aqueous ethidium bromide solution (0.5 $\mu\text{g}/\text{mL}$), and after that was visualized under UV light.

2.6.2. Interaction of the Co(III) complex (**2**) with a linear double-stranded DNA

Linear double-stranded lambda bacteriophage DNA (*cl857* Sam7, 48502 base pairs with a molecular weight of 31.5×10^6 Da) isolated from *E. coli* W3110 (purchased from Thermo Scientific, USA) was used in the experiments. DNA concentration and purity were confirmed spectrophotometrically. For agarose gel electrophoretic analysis, 0.3 μg of lambda DNA (0.01 pmol) was incubated with 5 nmol, 10 nmol or 15 nmol of the complex as described previously for plasmid DNA. For UV–Vis spectrometric analysis 500 μL of solution of lambda-DNA (0.5 pmol) in TS buffer were incubated at 37 $^\circ\text{C}$ for 2 h, vortexing from time to time, with different concentration of the complex (5 mM stock solution in DMSO). UV–Vis spectra were recorded at Shimadzu 1800 UV/Vis spectrometer.

3. Results and discussion

3.1. Synthesis

The reaction of 2-(diphenylphosphino)benzaldehyde and ethyl carbazate in ethanol at pH ~ 4 was performed and **1** was obtained. This ligand was used for preparation of Co(III) complex. Complex of Co(III) (**2**) was obtained by direct synthesis starting from $\text{Co}(\text{BF}_4)_2 \cdot 6\text{H}_2\text{O}$ and **1** (Fig. 1).

3.2. IR spectra

Comparison of IR spectra of ligand **1** and complex **2** indicates the complex formation. A new band appears in the complex at

1507 cm^{-1} originating from $\nu(\text{O}=\text{C}=\text{N})$ of the deprotonated hydrazide moiety, instead of the carbonyl band from uncoordinated ligand at 1707 cm^{-1} . In the bound ligand hydrazide nitrogen is deprotonated and as a consequence of electron delocalization $\text{C}=\text{O}$ bond acquires partial single bond character, and the $\text{C}-\text{N}$ bond partial double bond character. The $\text{B}-\text{F}$ band is located at 1060 cm^{-1} in the spectrum of **2**. This band originates from the tetrafluoroborate anion in the outer sphere of the complex.

3.3. NMR spectra

From the ^1H NMR spectrum of **2** (Table 3) it can be seen that the ligand is coordinated in monodeprotonated form, since the signal of hydrazide NH at 11.20 ppm is absent. Coordination via the imine nitrogen can be confirmed from ^1H NMR spectrum from the position of the signal of the imine carbon at 8.99 ppm which is shifted downfield in comparison to the corresponding signal in the ligand (8.71 ppm). In the ^1H NMR spectrum of **2** chemical shifts of aromatic protons have higher values, due to electron withdrawal by the coordinated metal ion. The signals of the methylene and methyl groups of the alcohol part of the ester are at 4.10 and 1.19 ppm, respectively in the ligand, and at 3.65 and 0.91 ppm, respectively in the complex.

Coordination through N1 results in a downfield shift of the hydrazone carbon C-3 (141.6 ppm in the spectrum of **1**; 155.4 ppm in the spectrum of **2**), and of the *para*-carbon C-7 (129.2 ppm in the spectrum of **1**; 133.7 ppm in the spectrum of **2**) (Table 4). There is a strong downfield shift of the carbonyl carbon C-14 due to coordination to Co(III), the signal is shifted from 153.4 ppm in the spectrum of **1** to 170.3 ppm in the spectrum of **2**. The consequence of coordination through phosphorus atom is the downfield shift of carbons *para* to phosphorus (C-6, C-13).

3.4. X-ray crystallographic analysis

Ligand **1** crystallizes with two independent molecules in the asymmetric unit of the monoclinic $I2/a$ space group (Fig. 2). The comparison of their bonding geometry with the average values found in the literature for similar compounds by using the program Mogul [29] shows that the molecular structures observed for **1** in

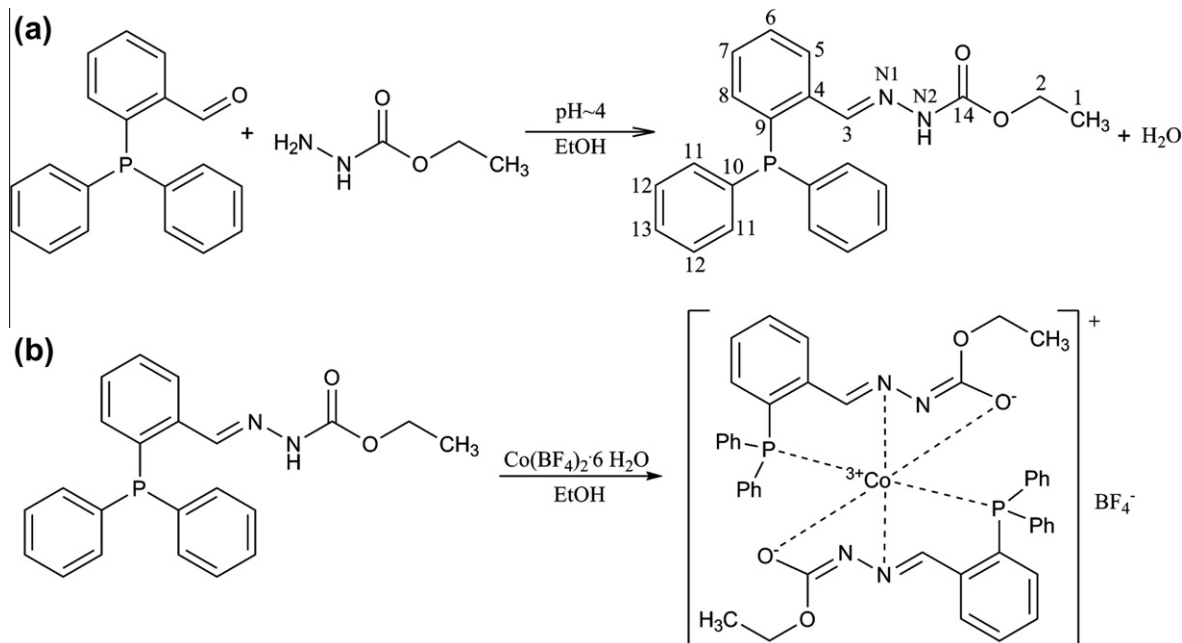


Fig. 1. (a) Synthesis of ligand **1**. (b) Synthesis of complex **2**.

Table 3
¹H NMR spectral data of **1** and **2**.

Assignment	Chemical shift (ppm), multiplicity, number of H-atoms, coupling constant <i>J</i> (Hz) for 1	Assignment	Chemical shift (ppm), multiplicity, number of H-atoms, coupling constant <i>J</i> (Hz) for 2
C1	1.19 (t, 3H, <i>J</i> = 7.1 Hz)	C1	0.91 (t, 3H, <i>J</i> = 7.0 Hz)
C2	4.10 (q, 2H, <i>J</i> = 7.0 Hz)	C2	3.47 (m, 1H)
		C2'	3.69 (m, 1H)
C3	8.71 (s, 1H)	C3	8.99 (s, 1H)
C5	6.80 (m, 1H)	C5	7.17 (m, 1H)
C6	7.31 (dt, 1H, <i>J</i> = 7.5 Hz, <i>J</i> = 1 Hz)	C6	7.51 (m, 1H)
C7	7.41 (m, 1H)	C7	7.86 (m, 1H)
C8	7.94 (m, 1H)	C8	8.05 (m, 1H)
C11	7.20 (m, 4H)	C11	7.22 (m, 2H)
		C11'	6.96 (m, 2H)
C12	7.41 (m, 4H)	C12	7.33 (m, 2H)
		C12'	7.11 (m, 2H)
C13	7.41 (m, 2H)	C13	7.51 (m, 1H)
		C13'	7.41 (m, 1H)
N2	11.20 (s, 1H)		

Table 4
¹³C NMR spectral data of **1** and **2**.

Assignment	¹³ C NMR chemical shift (ppm), coupling constant, <i>J</i> in Hz of 1	Assignment	¹³ C NMR chemical shift (ppm) of 2
C1	14.5	C1	14.0
C2	60.5	C2	65.4
C3	141.6	C3	155.4
C4	135.5, <i>J</i> = 10 Hz	C4	136.2
C5	132.9	C5	135.3
C6	129.6	C6	131.8
C7	129.2, <i>J</i> = 15 Hz	C7	133.7
C8	125.5, <i>J</i> = 3.75 Hz	C8	136.5
C9	135.6, <i>J</i> = 18.75 Hz	C9	136.1
C10	138.0, <i>J</i> = 18.75 Hz	C10	136.1
C11	133.5, <i>J</i> = 20 Hz	C11	133.8
		C11'	132.9
C12	128.8, <i>J</i> = 7.5 Hz	C12	128.1
		C12'	129.0
C13	129.1	C13	130.9
C14	153.4	C14	170.3

the solid state are not uncommon and their slightly different conformations evidenced in the inset suggest flexibility of the free ligand.

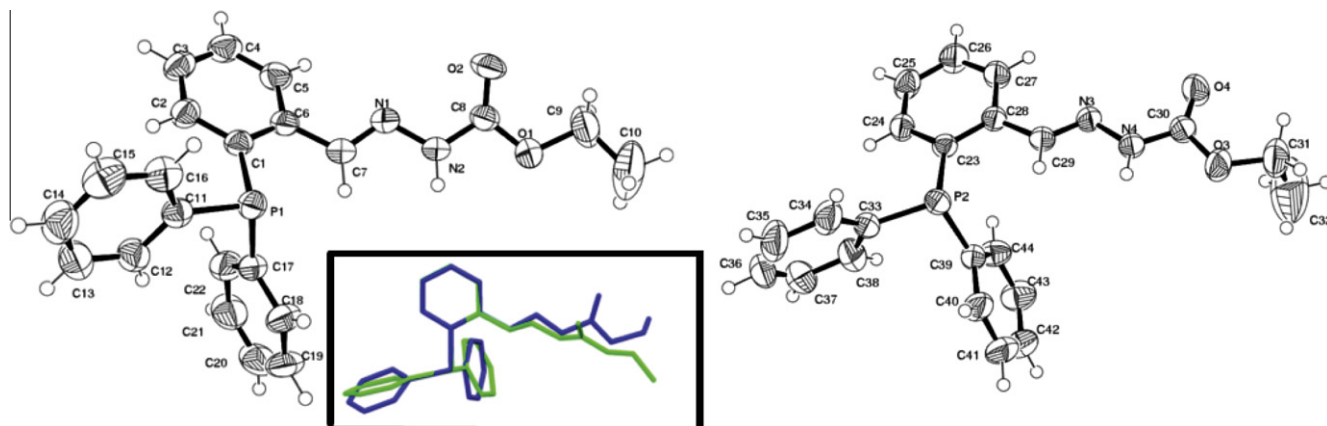


Fig. 2. Molecular structures and labeling of the two conformers observed in the crystal structures of **1**. In the inset the overlay of the two conformations is shown. Thermal ellipsoids are drawn at the 50% probability level.

Structures with $Z' > 1$ are in fact supposed to map the distribution of low energy conformers present in solution and kinetically frozen in the crystal [30]. The two conformations differ for small adjustments in the orientation of the phenyl rings, for the orientation of the terminal methyl group with respect to the NNHCOOCH₂ moiety and for the value of the torsion angle C5–C6–C7–N1 = 31° and C27–C28–C29–N3 = –6°. In both cases the imine nitrogen is pointing opposite to the phosphorous atom, but the orientation may be changed by rotation around the flexible C6–C7 bond in order to create a PN chelating system.

The ligand displays a conformational rearrangement around the C6–C7 bond upon coordination. In the cobalt(III) complex **2** two deprotonated ligand molecules coordinate the metal atom in a distorted octahedral geometry by chelation through the PNO donor system formed by the phosphorus, the imine nitrogen and the carbonyl oxygen (Fig. 3). Table 5 reports relevant bonding parameters for the complex. Apart from the slightly elongated Co–P distances, the remaining bond distances are not significantly different than the average observed for similar systems; however the chelation induces a strain on the bonding angular geometry of the two ligands. Namely the angles on the phosphorus atoms and on C7 and on C29 are wider than the average, while the angles N–C=O are smaller than usual, as evidenced by a comparison with similar systems performed by Mogul [29]. The C–O distance for the keto oxygen is now slightly elongated meaning that the negative charge is spread over more atoms, as in acetates. Fig. 3, inset, shows the points of maximum strain in the complex. The octahedral complex is in the *mer* configuration with an approximate molecular twofold symmetry, and the coordination implies the formation of two six-membered Co–P–C–C–N and two five-membered Co–N–N–C–O rings. These rings are practically planar, with puckering amplitudes close to zero: 0.03 Å for the ring containing P1, 0.16 for the one with P2, 0.07 for the ring comprising O3 and 0.19 for the one including O1. P2 and O1 are the atoms most deviating from planarity. The two chelation planes, comprising the atoms P–N–O–Co are practically perpendicular (dihedral angle = 87°). The octahedral complex cation in **2** is comparable with the complex containing a similar ligand, [bis(2-(diphenylphosphino)benzaldehyde benzoylhydrazone)-iron(III)]³⁺ (CSD refcode QEVYUM) [31] to which the structure of the cation in **2** is almost superimposable. Other two octahedral similar complexes have been described in the literature, namely bis(2-(diphenylphosphino)benzaldehyde benzoylhydrazone)-iron(II) tetrachloro-iron chloride (CSD refcode QEVYOG) [31] and bis(2-(diphenylphosphino)benzaldehyde benzoylhydrazone)-ruthenium(II) dimethyl sulfoxide solvate monohydrate (CSD refcode DEKJUZ) [32], but in these cases the two

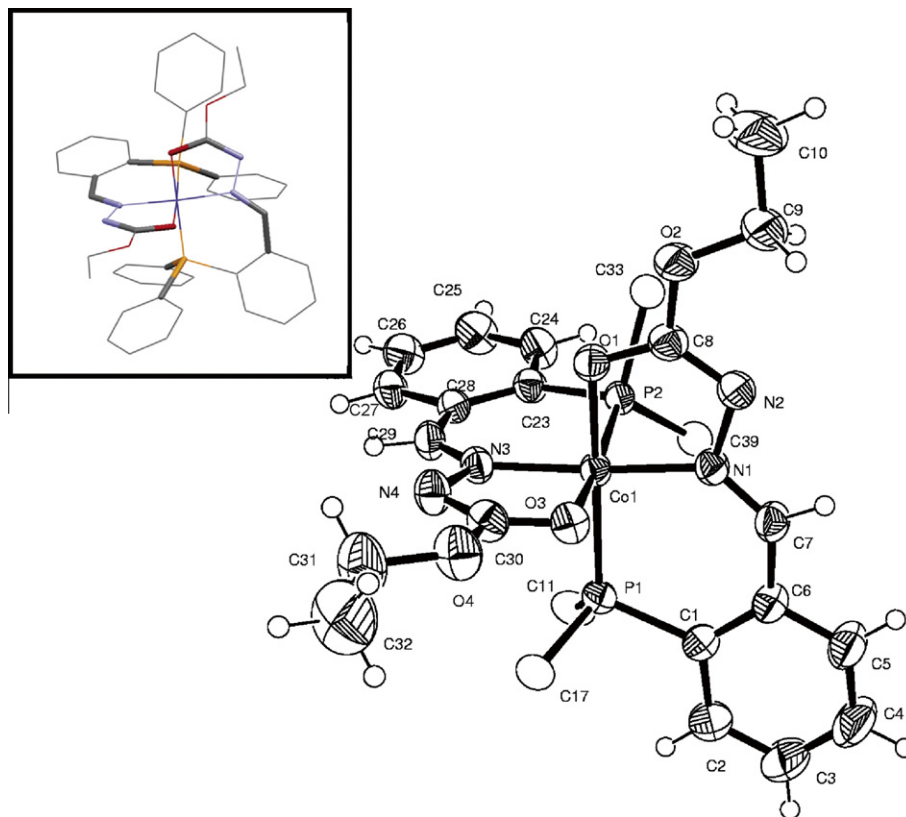


Fig. 3. Molecular structure of **2**, with labeling and thermal ellipsoids drawn at the 50% probability level. Phenyl groups attached to phosphorous atoms have been omitted for clarity and only the ipso carbon has been retained, shown in plain style. Inset: thick sticks indicate the main deformations of the molecular skeleton as compared to average values identified with Mogul [29].

Table 5
Most relevant bond lengths (Å) and angles (°) for **2**, with e.s.d.'s in parentheses.

Bond lengths			
Co1–P1	2.2541(4)	Co1–O3	1.928(1)
Co1–P2	2.2405(4)	Co1–N1	1.914(1)
Co1–O1	1.927(1)	Co1–N3	1.915(1)
Bond angles			
P1–Co1–P2	99.42(2)	O3–Co1–N1	88.08(5)
P1–Co1–O1	173.42(3)	O3–Co1–N3	83.23(5)
P1–Co1–O3	87.36(3)	N1–Co1–N3	168.24(5)
P1–Co1–N1	95.85(4)	Co1–P1–C2	110.94(5)
P1–Co1–N3	91.66(4)	Co1–P1–C11	121.00(5)
P2–Co1–O1	87.11(3)	Co1–P1–C17	111.18(5)
P2–Co1–O3	173.10(3)	Co1–P2–C24	111.42(5)
P2–Co1–N1	92.50(4)	Co1–P2–C33	114.32(5)
P2–Co1–N3	95.19(4)	Co1–P2–C39	115.51(5)
O1–Co1–O3	86.14(4)	Co1–O1–C8	108.43(9)
O1–Co1–N1	82.92(4)	Co1–O3–C30	107.95(9)
O1–Co1–N3	88.60(5)	Co1–N1–N2	112.71(9)
Co1–N1–C7	133.4(1)	Co1–N3–N4	112.47(9)
Co1–N3–C29	133.7(1)		

chelation systems are much less planar and P and O atoms deviate significantly from the average ligand planes.

The complex cation is counterbalanced by a BF_4^- anion orientationally disordered around the boron atom and the crystal packing does not reveal any significant structural motif.

3.5. Antimicrobial activity

The complex showed a strong activity to Gram positive bacteria, much higher than the activity of both the ligand and $\text{Co}(\text{BF}_4)_2 \cdot 6\text{H}_2\text{O}$ and similar to cefotaxime. The activity of the complex to Gram

negative bacteria was moderate, but again higher than both the ligand and the cobalt salt. The complex and the ligand were inactive to both strains of *C. albicans* (Table 6).

3.6. The brine shrimp test

The biological activity of **1** and **2** was tested by the brine shrimp test (toxicity to *A. salina*). The results of this test can be extrapolated to cell-line toxicity and anti-tumor activity [33,34]. The brine shrimp lethality test showed a moderate activity for **2** with LC_{50} 3.20 mM. The ligand and $\text{Co}(\text{BF}_4)_2 \cdot 6\text{H}_2\text{O}$ showed no activity.

3.7. Cytotoxic activity

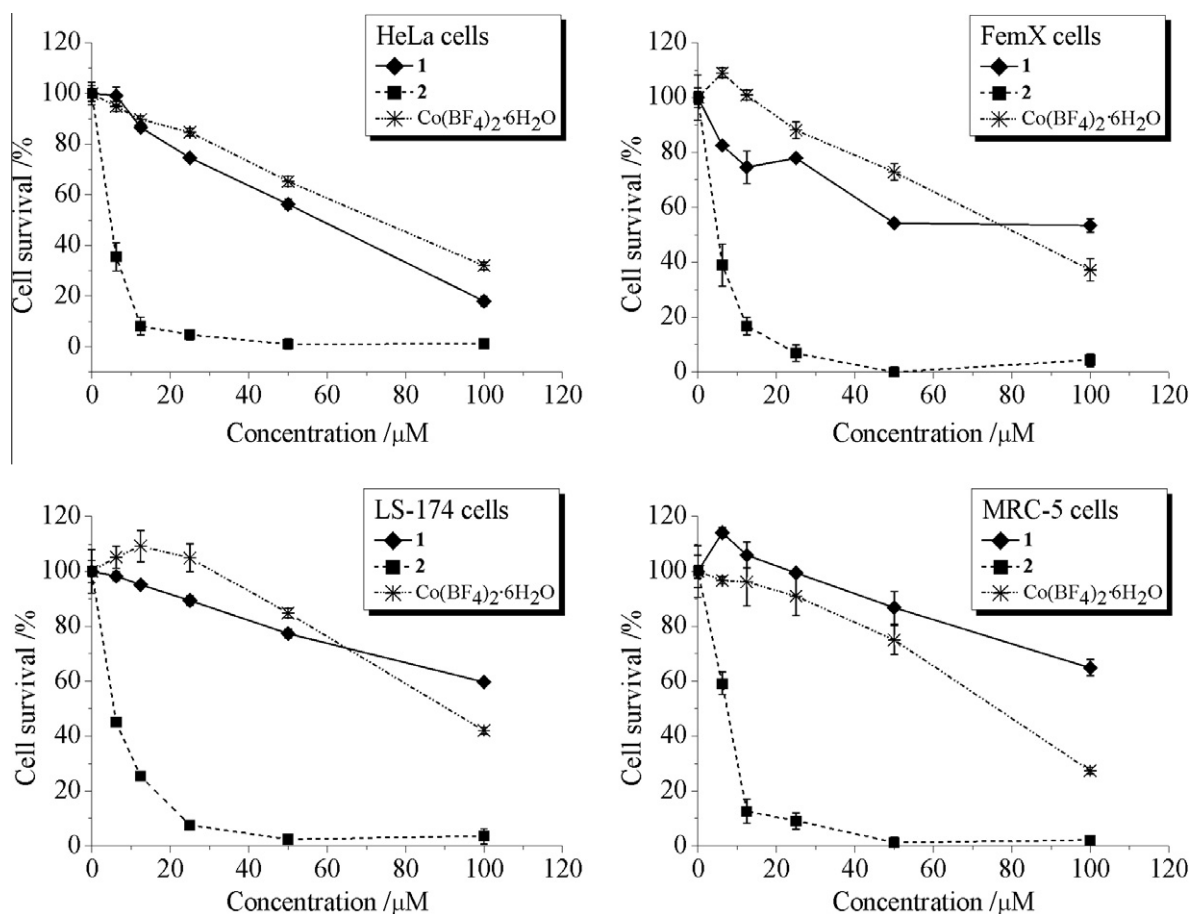
Cytotoxic activity of the investigated cobalt(III) complex (**2**), the ligand (**1**) and $\text{Co}(\text{BF}_4)_2 \cdot 6\text{H}_2\text{O}$ was determined by MTT assay after 48 h treatment of three tumor cell lines (HeLa, FemX and LS-174) and one normal cell line (MRC-5). Results are shown in Table 2 in terms of IC_{50} values. The complex (**2**) showed a very high cytotoxic activity, which was approximately twofold higher than cisplatin on cervix (HeLa), and melanoma tumor cell lines (FemX), and almost threefold higher in colorectal tumor cell line (LS-174), with IC_{50} values ranging from $4.90 \pm 0.08 \mu\text{M}$ (HeLa) to $7.42 \pm 2.45 \mu\text{M}$ (LS-174). Selectivity to HeLa cells was observed, both in regard to the other tumor cell lines and to the normal cell line. The ligand (**1**), when tested in the range of concentrations up to 100 μM , showed activity only to HeLa cells (IC_{50} value $58.28 \pm 0.23 \mu\text{M}$), which was twelve times lower than the activity of the complex. The cobalt(II) salt exhibited cytotoxic activity although to a much lower extent compared to the cobalt complex. The results are presented in terms of IC_{50} values that are deter-

Table 6

Minimal inhibitory concentration of the investigated compounds to selected microorganisms.

Microorganism	1 (mM) MIC	2 (mM) MIC	Co(BF ₄) ₂ ·6H ₂ O (mM) MIC	Cefotaxime (mM) MIC	Nystatin (μM) MIC
<i>Staphylococcus aureus</i> ATCC 25923	1.328	0.070	0.734	0.027	n.t.
<i>Staphylococcus epidermidis</i> ATCC 12228	1.328	0.070	0.367	0.027	n.t.
<i>Kocuria rhizophila</i> ATCC 9341	1.328	0.035	0.367	0.027	n.t.
<i>Bacillus subtilis</i> ATCC 6633	1.328	0.070	0.183	0.027	n.t.
<i>Escherichia coli</i> ATCC 25922	>1.328	0.279	0.367	0.007	n.t.
<i>Klebsiella pneumoniae</i> ATCC 13883	1.328	0.139	0.734	0.007	n.t.
<i>Pseudomonas aeruginosa</i> ATCC 27853	>1.328	0.139	0.367	0.027	n.t.
<i>Candida albicans</i> ATCC 10259	>1.328	>0.558	0.183	n.t.	0.216
<i>Candida albicans</i> ATCC 10231	>1.328	>0.558	0.183	n.t.	0.540

n.t.-not tested.

**Fig. 4.** Cell survival diagrams of HeLa, FemX, LS-174 and MRC-5 cells after 48 h of continual agent action for ligand (1), Co(III) complex (2) and cobalt salt. Data are representative for one out of three separate experiments with standard deviations.

mined from cell survival diagrams (Fig. 4). Values of IC₅₀ represent the average of two to three experiments, with each experiment performed in three replicates.

3.7.1. Cell cycle

The effect of investigated cobalt(III) complex on cell cycle progression of HeLa cells was examined by flow cytometry after con-

tinual treatment for 24 and 48 h, using staining with PI [26]. Examination of the histograms indicated that cobalt(III) complex induced perturbations of cell cycle of HeLa cells, results presented in Fig. 5. Obtained results show that cobalt(III) complex in HeLa cells induced decrease of percent of cells in G1 and slight increase of percent of cells in the S phase of cell cycle, with no important increase of apoptotic fraction of cells (evaluated as Sub-G1

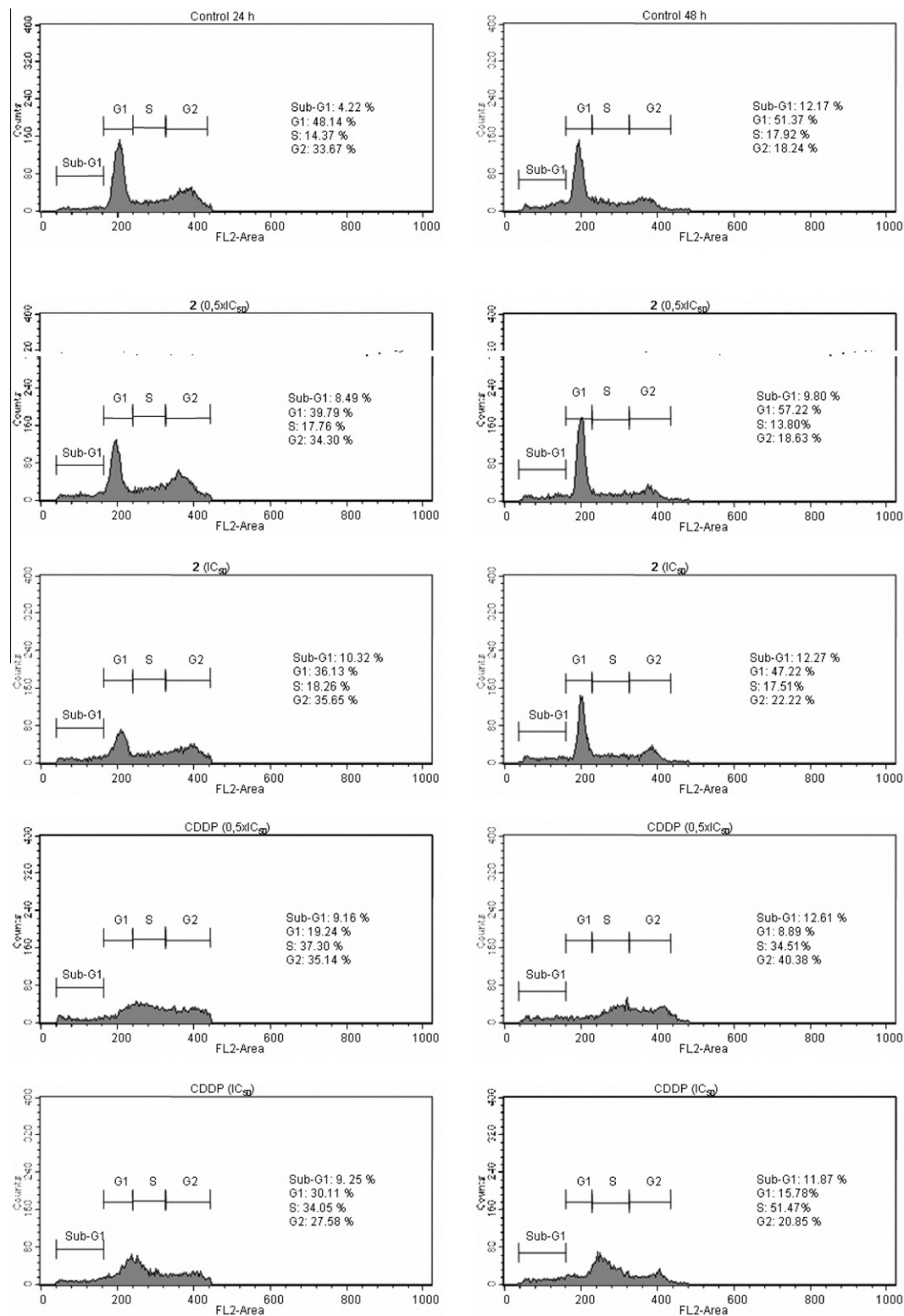


Fig. 5. Effect of Co(III) complex (**2**) and CDDP on cell cycle progression of HeLa cells following 24 and 48 h incubation with concentrations of investigated complexes corresponding to 0.5xIC₅₀ and IC₅₀. Control were untreated cells (incubated with nutrient medium only). Histograms presented are representative of three independent experiment.

fraction) after 24 h of continual agent action. Treatment for 48 h with the investigated complex indicated that cells that survived treatment were able to recover to normal cell cycle, indicating that

the investigated complex induced reversible interactions with DNA, in contrast to cisplatin which induced more permanent distortions of cell cycle.

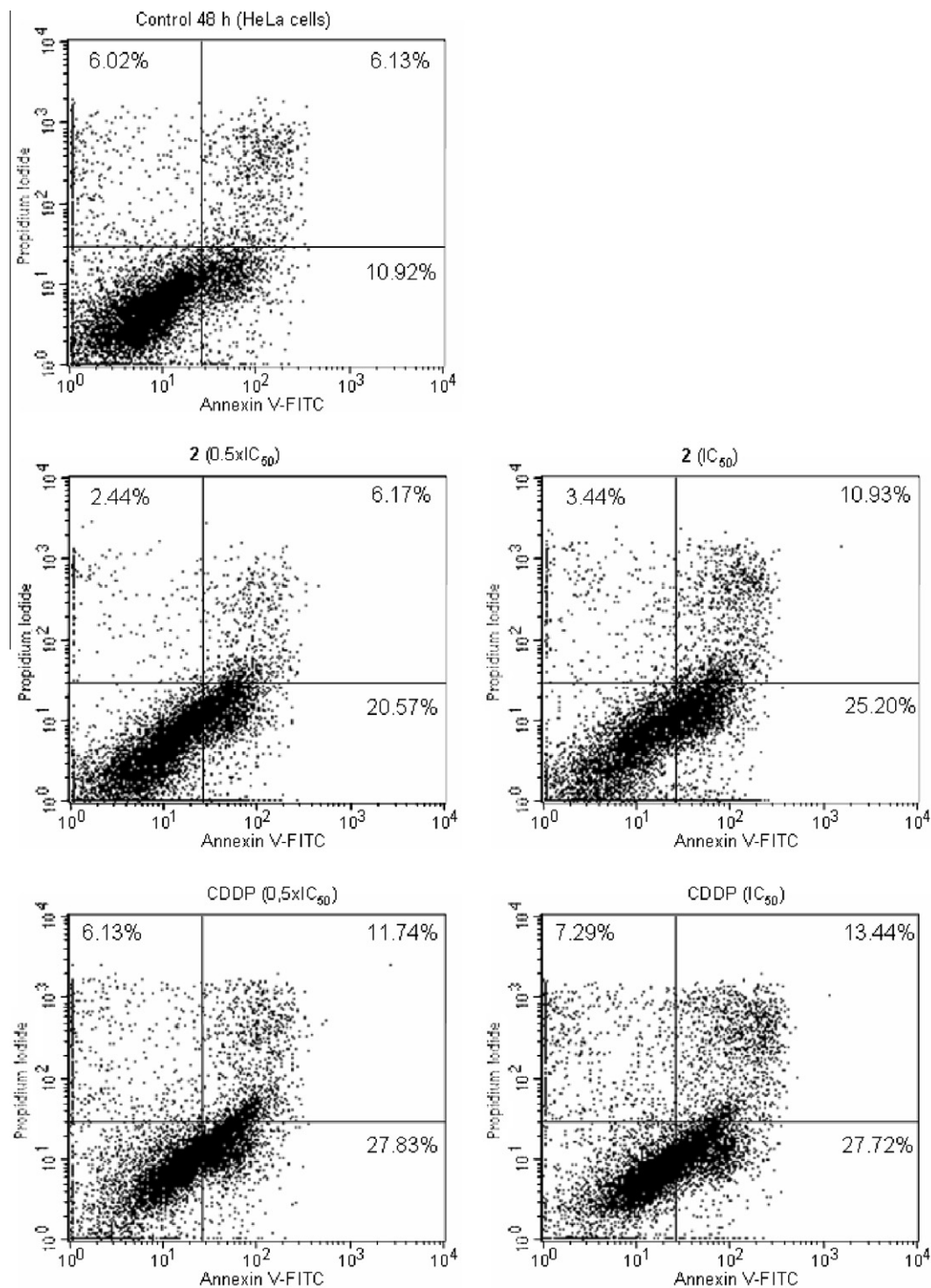


Fig. 6. Representative dot plot diagrams obtained by flow cytometry of Annexin-V-FITC/PI double-stained HeLa cells untreated (control) or treated with Co(III) complex (**2**) and CDDP with concentrations corresponding to $0.5 \times IC_{50}$ and IC_{50} . FITC(-)/PI(-) (lower-left quadrant) are intact cells, FITC(+)/PI(-) (lower-right quadrant) are early apoptotic cells, FITC(+)/PI(+) (upper-right quadrant) are late apoptotic or necrotic cells and FITC(-)/PI(+) (upper-left quadrant) are necrotic cells.

3.7.2. Apoptotic assay

Numerous studies of the molecular mechanisms of antitumor action of cisplatin pointed out that biochemical mechanisms of the cisplatin cytotoxicity involve the binding of the drug to DNA and non-DNA targets and further induction of cell death through apoptosis, necrosis or both within the heterogeneous population of cells that form a tumor mass [35,36]. Consequently, in investigating mechanism of action of newly synthesized metal complexes

it is crucial to consider interactions with DNA, through examination of cell cycle perturbations and potential of induction of apoptosis (determination of mode of cell death preferentially induced by investigated agent).

Potential of cobalt(III) complex (**2**) and CDDP to induce apoptotic cell death was determined by staining treated HeLa cells with two dyes Annexin V-FITC and propidium iodide and analysis on flow cytometer. Treatment with $0.5 \times IC_{50}$ and IC_{50} concentrations

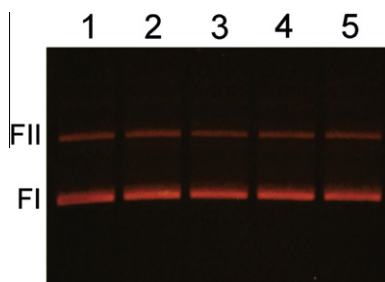


Fig. 7. Agarose gel electrophoresis showing no changes in electrophoretic mobility of the superhelical forms FII and the open circular forms FI of plasmid pUC18 DNA (0.13 pmol, lane 1) after incubation (1.5 h at 37 °C) with 5 nmol, 10 nmol and 15 nmol of the Co(III) complex (lanes 2, 3 and 4, respectively). The control sample: pUC18 (213 ng) with DMSO (3 μ L) (lane 5).

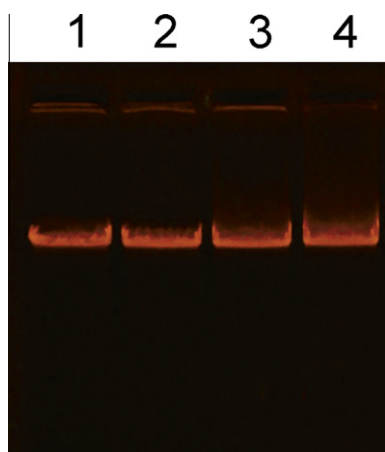


Fig. 8. Agarose gel electrophoresis showing damage of linear double-stranded lambda DNA (0.01 pmol, lane 1) after incubation (1.5 h at 37 °C) with 5 nmol, 10 nmol and 15 nmol of the Co(III) complex (lanes 2, 3 and 4, respectively).

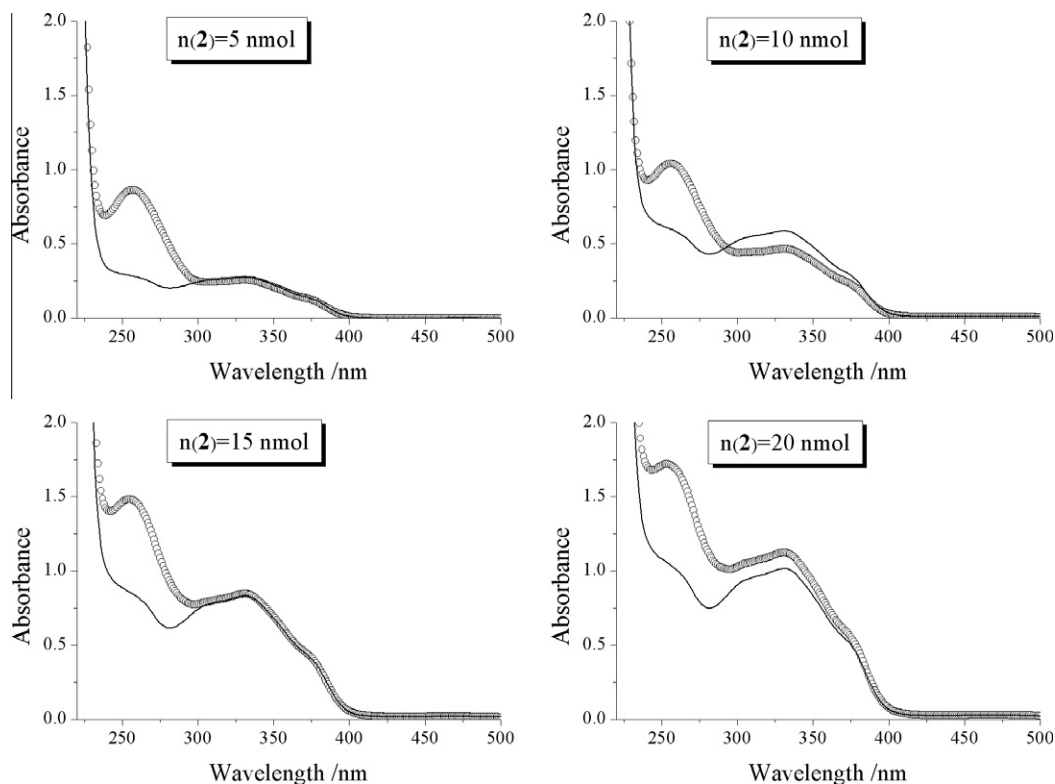


Fig. 9. Electronic absorption spectra of various amounts of the Co(III) complex in TS buffer after incubation (1.5 h at 37 °C) in the absence (lines) and the presence (circles) of lambda DNA (0.49 pmol).

of cobalt(III) complex and cisplatin for 48 h, induced similar percent of apoptotic cells for both complexes and with no differences between both concentrations (from 20% to 27%), Fig. 6.

3.8. DNA binding experiments

The interaction of metal complexes with double stranded closed circular plasmid DNA is usually monitored by agarose electrophoresis. The ability of Co(III) complexes to mediate DNA cleavage was well documented [37,38]. The effects of the Co(III) complex (2) on supercoiled DNA were studied using plasmid pUC 18 in TS buffer pH 7.9 (Fig. 7). The results showed that no strand scission was observed at increasing concentrations of the complex (Fig. 7, lanes 2, 3 and 4). The cleavage of plasmid DNA does not present a mode of action for this Co(III) complex, i.e., the complex has no nuclease activity. The result is in accordance with the previously obtained ones for dinuclear cobalt(III) complex with the condensation product of 2-acetylpyridine and malonic acid dihydrazide [39].

In order to test further cleavage efficiency of Co(III) complex, the complex was allowed to react with native linear double stranded bacteriophage lambda DNA for 1.5 h at 37 °C. It can be seen from the electrophoregram in Fig. 8 that the complex again did not show a noticeable DNA cleavage activity. Binding of the complex to the DNA causes the DNA bands to smear in the gel (lanes 2–4). The changes in DNA bands were observed in a concentration-dependent way.

Spectroscopic methods were employed to further ascertain whether there is any binding of the complex with bacteriophage lambda DNA. Electronic absorption spectra of the complex in aqueous buffer media both in the absence and the presence of lambda DNA are given in Fig. 9.

It can be seen that there are minimal changes in spectroscopic patterns, indicating no binding of the complex to lambda DNA. The observations are in accordance with the results of cell cycle and apoptosis experiments.

4. Conclusions

The newly synthesized complex showed a strong cytotoxic activity to the tested cell lines with selectivity to HeLa cells. The Pt(II) and Pd(II) complexes with similar ligands also showed a strong cytotoxic activity [19], but with a different mechanism of action. The investigated Co(III) complex had a different effect on cell cycle progression of HeLa cells than either of the three previously studied complexes [19] or cisplatin. Namely, it caused no important increase of apoptotic (sub-G1) fraction. Contrary to cisplatin the effects on cell cycle progression were temporary. On the other hand, in the Annexin V–FITC apoptosis test, for detection of one marker of early apoptosis, externalization of phosphatidylserine, the newly synthesized complex, cisplatin and the previously synthesized complexes showed similar effects. High cytotoxicity of cobalt(III) complex and low perturbations of cell cycle, moderate potential of induction of externalization of phosphatidylserine and insignificant spectral and electrophoretical changes indicate that DNA is not the target responsible for cytotoxicity of this complex.

Acknowledgements

Financial support of the Ministry of Education and Science of the Republic of Serbia (Grant OI 172055 and Grant III 41026).

Appendix A. Supplementary material

CCDC 883135 and 883136 contains the supplementary crystallographic data for this paper. These data can be obtained free of charge from The Cambridge Crystallographic Data Centre via www.ccdc.cam.ac.uk/data_request/cif. Supplementary data associated with this article can be found, in the online version, at <http://dx.doi.org/10.1016/j.ica.2012.09.043>.

References

- [1] P.N. Liu, F.H. Su, T.B. Wen, H.H.Y. Sung, I.D. Williams, G. Jia, *Chem. Eur. J.* 16 (2010) 7889.
- [2] C. Sui-Seng, F.N. Haque, A. Hadzovic, A. Pütz, V. Reuss, N. Meyer, A.J. Lough, M. Zimmer-De Iuliiis, R.H. Morris, *Inorg. Chem.* 48 (2009) 735.
- [3] D.B.G. Williams, M. Pretorius, *J. Mol. Catal. A: Chem.* 284 (2008) 77.
- [4] S.J. Degrado, H. Mizutani, A.H. Hoveyda, *J. Am. Chem. Soc.* 124 (2002) 13362.
- [5] D.M. Mampreian, A.H. Hoveyda, *Org. Lett.* 6 (2004) 2829.
- [6] C.Z. Flores-López, L.Z. Flores-López, G. Aguirre, L.H. Hellberg, M. Parra-Hake, R. Somanathan, *J. Mol. Catal. A: Chem.* 215 (2004) 73.
- [7] H. Dai, X. Hu, H. Chen, C. Bai, Z. Zheng, *J. Mol. Catal. A: Chem.* 209 (2004) 19.
- [8] E.L. Carswell, M.L. Snapper, A.H. Hoveyda, *Angew. Chem., Int. Ed.* 45 (2006) 7230.
- [9] J. Wencel, D. Rix, T. Jennequin, S. Labat, C. Crévisy, M. Mauduit, *Tetrahedron: Asymmetry* 19 (2008) 1804.
- [10] S.D. Phillips, J.A. Fuentes, M.L. Clarke, *Chem. Eur. J.* 16 (2010) 8002.
- [11] S.B. Novakovic, G.A. Bogdanovic, I.D. Brceski, V.M. Leovac, *Acta Crystallogr. C* 65 (2009) 263.
- [12] V.M. Leovac, B. Ribár, G. Argay, A. Kálmán, I. Brčeski, *J. Coord. Chem.* 39 (1996) 11.
- [13] G. Argay, A. Kálmán, L. Párkányi, V.M. Leovac, I.D. Brceski, P.N. Radivojsa, *J. Coord. Chem.* 51 (2000) 9.
- [14] I.D. Brceski, V.M. Leovac, G.A. Bogdanovic, S.P. Sovilj, M. Revenco, *Inorg. Chem. Commun.* 7 (2004) 253.
- [15] A. Bacchi, M. Carcelli, M. Costa, A. Leporati, E. Leporati, P. Pelagatti, C. Pelizzi, G. Pelizzi, *J. Organomet. Chem.* 535 (1997) 107.
- [16] P. Pelagatti, A. Bacchi, M. Carcelli, M. Costa, A. Fochi, G. Ghidini, E. Leporati, M. Masi, C. Pelizzi, G. Pelizzi, *J. Organomet. Chem.* 583 (1999) 94.
- [17] A. Bacchi, M. Carcelli, M. Costa, A. Fochi, C. Monici, P. Pelagatti, C. Pelizzi, G. Pelizzi, L.M.S. Roca, *J. Organomet. Chem.* 593–594 (2000) 180.
- [18] V. Radulovic, A. Bacchi, G. Pelizzi, D. Sladic, I. Brceski, K. Andjelkovic, *Monatsh. Chem.* 137 (2006) 681.
- [19] N. Malesevic, T. Srdic, S. Radulovic, D. Sladic, V. Radulovic, I. Brceski, K. Andjelkovic, *J. Inorg. Biochem.* 100 (2006) 1811.
- [20] SAINT: SAX, Area Detector Integration, Siemens Analytical instruments INC., Madison, Wisconsin, USA. SADABS: Siemens Area Detector Absorption Correction Software, G. Sheldrick, 1996, University of Goettingen, Germany.
- [21] A. Altomare, M.C. Burla, M. Cavalli, G. Cascarano, C. Giacovazzo, A. Gagliardi, A.G. Moliterni, G. Polidori, R. Spagna, Sir97: A new Program for Solving and Refining Crystal Structures, Istituto di Ricerca per lo Sviluppo di Metodologie Cristallografiche CNR, Bari, 1997.
- [22] G. Sheldrick, Shelxl97, Program for structure refinement, University of Goettingen, Germany, 1997.
- [23] (a) L.J. Farrugia, *J. Appl. Crystallogr.* 32 (1999) 837; (b) M. Nardelli, *J. Appl. Crystallogr.* 28 (1995) 659.
- [24] (a) F.H. Allen, O. Kennard, R. Taylor, *Acc. Chem. Res.* 16 (1983) 146; (b) I.J. Bruno, J.C. Cole, P.R. Edgington, M. Kessler, C.F. Macrae, P. McCabe, J. Pearson, R. Taylor, *Acta Crystallogr. B* 58 (2002) 389.
- [25] R. Supino, in: S. O'Hare, C.K. Atterwill (Eds.), *Methods in Molecular Biology, In Vitro Toxicity Testing Protocols*, Humana Press, New Jersey, 1995, pp. 137–149.
- [26] M.G. Ormerod, in: M.G. Ormerod (Ed.), *Analysis of DNA-General Methods: Flow Cytometry a Practical Approach*, Oxford University Press, New York, 1994, pp. 119–125.
- [27] W.J. Dower, J.F. Miller, C.W. Ragsdale, *Nucleic Acid Res.* 16 (1988) 6127.
- [28] H.C. Birnboim, J. Doly, *Nucleic Acid Res.* 7 (1979) 1513.
- [29] I.J. Bruno, J.C. Cole, M. Kessler, J. Luo, W.D.S. Motherwell, L.H. Purkis, B.R. Smith, R. Taylor, R.I. Cooper, S.E. Harris, A.G. Orpen, *J. Chem. Inf. Comput. Sci.* 44 (2004) 2133.
- [30] (a) H.B. Bürgi, J.D. Dunitz, *Acc. Chem. Res.* 16 (1983) 153; (b) G.R. Desiraju, *Cryst. Eng. Commun.* 91 (2007) 91.
- [31] P. Pelagatti, A. Bacchi, M. Balordi, A. Caneschi, M. Giannetto, C. Pelizzi, L. Gonsalvi, M. Peruzzini, F. Ugozzoli, *Eur. J. Inorg. Chem.* 2007 (2007) 162.
- [32] P. Pelagatti, A. Bacchi, M. Balordi, S. Bolaño, F. Calbiani, L. Elviri, L. Gonsalvi, C. Pelizzi, M. Peruzzini, D. Rogolino, *Eur. J. Inorg. Chem.* 2006 (2006) 2422.
- [33] B.N. Meyer, N.R. Ferrigni, J.E. Putnam, L.B. Jacobsen, D.E. Nichols, J.L. McLaughlin, *Planta Med.* 45 (1982) 31.
- [34] J.E. Anderson, C.M. Goetz, J.L. McLaughlin, M. Suffness, *Phytochem. Anal.* 2 (1991) 107.
- [35] V. Cepeda, M.A. Fuertes, J. Castilla, C. Alonso, C. Quevedo, J.M. Pérez, *Anti-Cancer Agents Med. Chem.* 7 (2007) 3.
- [36] G. Hortobagyi, *Semin. Oncol.* 25 (1998) 1.
- [37] R.S. Kumar, S. Arunachalam, V.S. Periasamy, C.P. Preethy, A. Riyasdeen, M.A. Akbarsha, *Polyhedron* 27 (2008) 1111.
- [38] P. Nagababu, J.N.L. Latha, Y. Prashanthi, S. Satyanarayana, *J. Chem. Pharm. Res.* 1 (2009) 238.
- [39] R. Eshkourfu, B. Čobeljić, M. Vujčić, I. Turel, A. Pevec, K. Sepčić, M. Zec, S. Radulović, T. Srdić-Radić, D. Mitić, K. Andjelković, D. Sladić, *J. Inorg. Biochem.* 105 (2011) 1196.